RSC Advances

PAPER

View Article Online
View Journal | View Issue

Cite this: *RSC Adv.*, 2018, **8**, 23181

Bioassay-guided isolation and identification of anticancer and antioxidant compounds from *Gynostemma pentaphyllum* (Thunb.) Makino

Tian-Xing Wang, Man-Man Shi and Jian-Guo Jiang *

Gynostemma pentaphyllum (Thunb.) Makino is a medicinal and edible plant in China whose buds and leaves are used for making a popular kind of tea drink. The anticancer and antioxidant properties of the ethyl acetate (EA) and *n*-butanol (*n*-Bu) fractions provide a basis for conducting experiments for isolation and identification of key compounds that may be responsible for the aforementioned properties of *G. pentaphyllum*. Four compounds were isolated from the two fractions using ODS packing column, silica gel column, polyamide column, Sephadex LH-20 gel column and HPLC. With the aid of ^{1}H, ^{13}C NMR and mass spectrometry, they were identified as 3,4-dihydroxy phenyl-*O*-β-D-glucoside, gypenoside XLVI, gypenoside L and ginsenoside Rd. 3,4-Dihydroxy phenyl-*O*-β-D-glucoside showed the strongest DPPH (97.23%) and ABTS (101.37%) scavenging effect and ferric ion reducing power (FRAP value 0.8846), which may be closely related to the hydrogen atoms of phenolic hydroxyls. Gypenoside L and ginsenoside Rd displayed the highest inhibition of tumor cell proliferation of A549 and MCF-7 cell lines, which had to do with the chemical structure of the compounds bearing glycosylated parts and free hydroxyls at the 20th or 21st carbon atom of dammarane-type saponin.

Received 1st April 2018
Accepted 29th May 2018

DOI: 10.1039/c8ra02803f

rsc.li/rsc-advances

1. Introduction

Gynostemma pentaphyllum (Thunb.) Makino belongs to the family Cucurbitaceae and is widely distributed in China, Japan and other Asian countries.[1] As a cultivated plant with medicinal properties and edibility,[2] it was traditionally used to reduce inflammation, relieve cough and eliminate phlegm in traditional medicine prescriptions.[3] Also, some popular tea drinks have been made from its buds and leaves.[4] There are several autopolyploid species of *G. pentaphyllum* whose chemical composition and health characteristics are different.[5] The dammarane gypenosides are considered as the major bioactive constituents in *G. pentaphyllum*.[6] To date, approximate 180 gypenosides have been isolated from it, which display various bioactivities such as hepatoprotective,[7] antioxidant,[8] anti-obesity,[9] anti-inflammatory,[10] hypolipemic,[11] hypoglycemic,[12] and anticancer properties.[13]

Free radicals are molecules/molecular fragments containing one or more unpaired electrons, the presence of which usually makes them highly reactive.[14] Previous studies have shown that the damage of cells caused by free radicals played a key role in the etiology of a wide range of human diseases,[15] including arthritis, hemorrhagic shock, coronary artery diseases, cataract, cancer, AIDS as well as age-related degenerative brain diseases. Recent evidence reports that cancer cells persistently exhibit high ROS levels as a result of metabolic, genetic and microenvironment-associated alterations.[16,17] Increased levels of ROS are pro-tumorigenic, resulting in the activation of pro-survival signaling pathways, loss of tumor suppressing gene-function, increased glucose metabolism, adaptations to hypoxia, and the generation of oncogenic mutations,[18] suggesting that antioxidants may have an anticancer effect by preventing the build-up of excessive ROS.

The safety and toxicity of synthetic antioxidants are of concern.[19] At present, cancer treatment is mainly based on western medicine which is characterized by addiction, drug resistance and complex adverse reactions.[20] Now, researchers are interested in developing plant-derived drugs with low toxicity and side effects.[21,22]

Antioxidant and anticancer effect of different crude extracts from *G. pentaphyllum* were investigated systematically, although only a few reports have discussed the activity of individual compounds in *G. pentaphyllum* and their separation method. Considering this limited background, the present study focused on the bioassay-guided isolation and purification of active individual compounds from *G. pentaphyllum*. 1,1-Diphenyl-2-picrylhydrazyl (DPPH), 2,2′-azino-bis(3-ethylbenzothiazoline-6-sulfonic acid) (ABTS) and ferric ion reducing antioxidant power (FRAP) were applied for the antioxidant capacity. Normal liver cell lines, LO2, were applied for the cytotoxicity evaluation of crude extracts and compounds, and their anticancer effect against two

College of Food and Bioengineering, South China University of Technology, Guangzhou, 510640, China. E-mail: jgjiang@scut.edu.cn; Fax: +86-20-87113843; Tel: +86-20-87113849

human tumor cell lines, mammary gland breast cancer, MCF-7, and human non-small cell lung carcinoma, A549, were analyzed.

2. Materials and methods

2.1 Reagents and chemicals

TPTZ (tripyridyltriazine), DPPH (1,1-diphenyl-2-picrylhydrazyl) and ABTS (2, 2′-azino-bis(3-ethylbenzothiazoline-6-sulfonic acid)) were purchased from Sigma-Aldrich (Darmstadt, Germany). Phosphoric acid, methanol-D4, chloroform-d, DMSO (Dimethyl Sulfoxide)-D6 were purchased from Aladdin. Analytical-grade methanol, ethanol, petroleum ether (PE), ethyl acetate (EA), chloroform and *n*-butanol (*n*-Bu), in addition to HPLC-grade acetonitrile, methanol were purchased from Shanghai Macklin Biochemical Co, Ltd. Potassium ferricyanide, trichloroacetic acid, ferric chloride, potassium persulfate, hydrochloric acid were of analytical grades.

2.2 Preparation of different polar fractions

Dried whole herbs of *G. pentaphyllum*, originally from Pingli, Shaanxi Province, were purchased from a Chinese medicinal materials market in Guangzhou and identified by researcher Deng Yunfei of South China Botanical Garden, Chinese Academy Sciences. Different polar fractions were obtained as shown in Fig. 1 after ordinal treatment with petroleum ether, chloroform, ethyl acetate and *n*-butanol.

2.3 Isolation and purification of EA fraction and *n*-Bu fraction

As shown in Fig. 1, EA fraction (30 g) was separated using a silica gel (200–300 mesh) column chromatography using chloroform–methanol gradient elution method to obtain three fractions. For further isolation, fraction 1 was exposed to a Sephadex LH-20 gel column using methanol–H_2O (70 : 30, v/v). Polyamide column chromatography (methanol–H_2O = 40 : 60, v/v) was used for further purification to obtain compound **1** (20 mg). Using silica gel (200–300 mesh) column chromatography with a chloroform–methanol solvent system, *n*-Bu fraction (45 g) was divided into four fractions as shown in Fig. 1. Fraction 2 was repeatedly subjected to Sephadex LH-20 gel column with methanol : H_2O (70 : 30, v/v) as elution solvent. After continuous processing with ODS column (methanol : H_2O = 70 : 30, v/v) and silica gel column (chloroform–methanol = 3 : 1, v/v), compound **2** was obtained from fraction 2-2-1 (270 mg). Fraction 4 was exposed to Sephadex LH-20 gel column with methanol. For further purification, ODS column chromatography with methanol : H_2O (60 : 40, v/v) as the elution solvent was used to obtain fraction 3-1-1. After treatment with silica gel column using chloroform–methanol (2 : 1, v/v), compound **3**

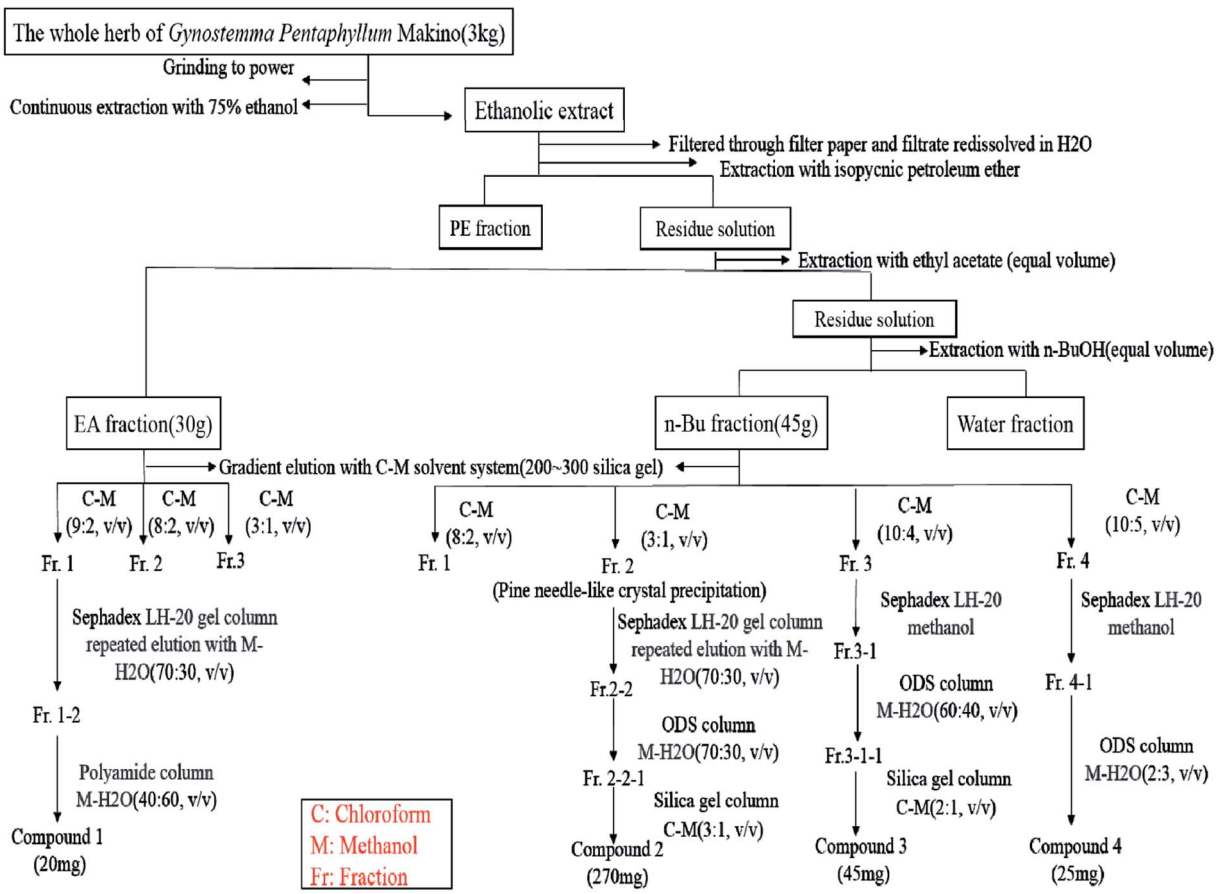

Fig. 1 Preparation of different polar fractions and isolation and purification of EA fraction and *n*-Bu fraction.

was chromatographed from fraction 3-1-1. Fraction 4 was purified twice with Sephadex LH-20 column chromatography using methanol as the elution solvent. The target compound present in fraction 4 was mainly enriched in fraction 4-1, and then further purified by ODS column chromatography to obtain compound **4**.

2.4 Antioxidant assays

2.4.1 DPPH scavenging capacity assay. The lone pair electrons in DPPH were bound by protons under the presence of free radical scavenger, thus lightening the color and reducing the photoabsorption of reaction solution.[23] To varying concentrations of 180 μL of DPPH standard solution (0, 30, 90, 150, 210, 240, 270 μg mL^{-1}), 20 μL of absolute ethanol was added and reacted away from light for 30 min, establishing the standard curve. The concentration with absorbance of 0.7–0.8 was selected as the concentration of the working fluid. Then, 20 μL of samples at different concentration (25–800 μg mL^{-1}) were mixed with 180 μL of DPPH working solution. After 30 min of incubation in the dark, the absorbance was calculated in a microplate reader at 518 nm. The ABTS scavenging capacity was calculated by the equation below:

$$\text{DPPH}^{\cdot}\text{ scavenging capacity (\%)} = [1 - (A_b - A_c)/A_d] \times 100$$

where A_b is the sample absorbance, A_c is the background absorbance and A_d is the control absorbance.

2.4.2 ABTS scavenging capacity assay. The absorption spectra of the various samples at 737 nm was positively controlled with ascorbic acid and used to evaluate ABTS radical scavenging capacity of various samples based on the published report.[24] Initially, aqueous (7 mM) ABTS and potassium persulfate solutions (4.9 mM) were mixed in equal volumes and stored under a cool and dark condition. ABTS mother liquor was diluted with absolute ethanol to obtain an absorbance of 0.70 ± 0.020 at 737 nm. Then, 20 μL of various samples of different concentrations (25–800 μg mL^{-1}) was put in 96-well plates, followed by adding 180 μL of diluted ABTS solution. The absorbance was measured at 737 nm, and ABTS scavenging capacity was calculated according to the equation below.

$$\text{ABTS}^{\cdot+}\text{ clearance (\%)} = [1 - (A_b - A_c)/A_d] \times 100$$

in which, A_b, A_c and A_d are the sample, background and control absorbance, respectively.

2.4.3 Ferric reducing antioxidant power (FRAP) assay. Fe^{3+}–TPTZ was reduced by an electronating agent and formed Fe^{2+}–TPTZ at low pH.[25] The working solution was prepared by mixing acetate buffer (0.3 M, pH 3.6), TPTZ solution (10 mM) and ferric chloride solution (20 mM) (10 : 1 : 1, v/v/v). Then, 20 μL of samples with different concentrations (25–800 μg mL^{-1}) were mixed with 180 μL of FRAP working solution. Upon treatment of the vortex and incubation for 30 min, the absorbance of the mixture was measured at 596 nm accurately. With $FeSO_4$ as the standard solution, the antioxidant activity of the sample is expressed as the $FeSO_4$ concentration that reached the same absorption value, that is, the FRAP value of all tested samples.

2.5 Anticancer assays

2.5.1 Cell culture and cytotoxicity assay. The cytotoxicity of samples was investigated on LO2 cell lines (normal liver cell). The anticancer capacity of all tested samples was observed on human breast adenocarcinoma cell lines (MCF-7) and human alveolar adenocarcinoma cell lines (A549), which were purchased from the Chinese Academy of Science Cell Bank. These cells were maintained in DMEM high glucose culture fluid (Gibco Company, USA), supplemented with 10% fetal bovine serum, 0.5% streptomycin (Gibco Company, USA) and 0.5% penicillin (Gibco Company, USA) in a cell incubator at 37 °C with 5% CO_2.

2.5.2 MTT assay for inhibition rate of cell proliferation. The cell viability of these cell lines was measured by MTT assay.[26] Briefly, all tested samples and the standard were dissolved with DMSO adequately, preparing the stock solution (40 mg mL^{-1}) with a limited percentage (1%) of DMSO-usage. Using a doubling dilution method, the stock solution was diluted to a series of concentrations (25–800 μg mL^{-1}) by DMEM high glucose culture fluid supplemented with 10% fetal bovine serum, 0.5% streptomycin and 0.5% penicillin. 100 μL of cells in logarithmic growth phase (3×10^4 cells per mL) per well were inoculated in a 96-well plate and cultured for 24 h. Then, 100 μL of diluted sample medium was added to replace the old nutrient fluid and incubated for 24 h. The complete medium and 5-F, instead of sample solution, were used as blank control group and positive control group, respectively. Thereafter, 100 μL of DMEM high glucose culture fluid and 20 μL MTT regent (5 mg mL^{-1}) was added to replace the old medium and cultured for 4 h. Next, the medium containing MTT was abandoned, followed by adding 150 μL DMSO per well to dissolve the formazan crystals. After shaking for 10 min, the OD value was measured with a microplate reader at 490 nm. The cell proliferation inhibition rate was calculated by the equation below.

$$\text{Inhibition rate (\%)} = (1 - \text{OD}_{\text{sample}}/\text{OD}_{\text{control}}) \times 100$$

2.6 Statistical analysis

All experiments were performed in triplicate, and the data were expressed as mean ± standard deviation (SD). Statistical differences were evaluated by one-way analysis of variation using SPSS 17.0 with Bonferroni correction. Significant differences were revealed at $P < 0.05$.

3. Results and discussion

3.1 Identification of isolated compounds

Compound **1** was obtained as yellow powder with lyophilization treatment and developed with methanol–H_2O (1 : 1, v/v) in a polyamide thin sheet. A single yellow fluorescence spot was presented under 254 nm UV irradiation after heating. ESI-MS (m/z): 288, ^{1}H-NMR (400 MHz, DMSO-d_6): δ_H 8.91 (1H, s, OH), 8.49 (1H, s, OH), 6.59 (1H, d, J = 8.5 Hz, H-5), 6.47 (1H, d, J =

2.7 Hz, H-2), 6.32 (1H, dd, $J = 8.5$, 2.7 Hz, H-6), 5.23 (1H, d, $J =$ 4.4 Hz, OH), 5.02 (1H, d, $J = 5.1$ Hz, OH), 4.59 (1H, d, $J = 7.5$ Hz, H-1′), 4.54 (1H, s, OH), 3.65 (1H, dd, $J = 11.0$, 1.5 Hz, H-6′), 3.45 (1H, m, H-6′), 3.17 (4H, m, H-2′,-3′,-4′,-5′). ^{13}C-NMR (DMSO-d_6) δ_C 150.8(d), 145.6(s), 140.3(s), 115.5(d), 106.8(d), 105.4(d), 101.8(d), 76.9(d), 76.7(d), 73.4(d), 69.8(d), 60.8(t). Based on these data (Fig. 2A) and a previously published report,[27] compound **1** was determined to be 3,4-dihydroxy phenyl-*O*-β-D-glucoside.

Compound **2** was obtained as a white needle-like crystalline powder. A bright yellow brown spot was introduced by using chloroform : methanol : H_2O in 3.5 : 1 : 0.2 ratio in a silica gel plate. After the color faded, a purple luminous point emerged using an alcoholic solution of sulfuric acid (10%) as coloring agent and heating to 105 °C. ESI-MS *m*/*z*: 961.5346 ($C_{48}H_{82}O_{19}$). The ^{1}H-NMR spectrum (Fig. 2B) showed eight signals for methyl protons, three glycosyl hydrogen signals and one tri-substituted allyl stromal signal that corresponded with the structure. According to the coupling constant of glycosyl hydrogen (7.6, 7.6, 7.8 Hz), the glycoside configuration was determined to be of the β-type. The ^{13}H-NMR spectrum revealed 48 signals containing two alkenyl carbon atoms (δ_C 132.28, 125.86). According to these results and the reported literature,[28] compound **2** was determined to be gypenoside XLVI.

Compound **3** was obtained a white shapeless powder. Using the chloroform–methanol–H_2O (3 : 1 : 0.2, v/v/v) developing system, there was no obvious UV absorption at 254 nm and 365 nm ultraviolet light. ESI-MS *m*/*z*: 799. The ^{1}H-NMR and ^{13}C-NMR spectrum (Fig. 2C) are very similar to that of compound **4**. The only difference is that signals observed at δ_C of 57.23, 72.06, 27.28, 35.71 ppm were attributed to the glucoside structure, revealing that the absolute configuration of C-20 belongs to the S conformer. The spectral data were in accordance with the literature,[29] and the compound **3** was identified as gypenoside L.

Compound **4** was obtained as a white amorphous powder. Using the chloroform–methanol–H_2O (3 : 0.8 : 0.16, v/v/v) developing system, there was no obvious UV absorption at 254 nm and 365 nm ultraviolet light. A bright yellow brown spot emerged in the silica gel plate that was placed in the iodine cylinder. After the color faded, a purple bright point was obtained using an alcoholic solution of sulfuric acid (10%) as the coloring agent and by heating to 105 °C. ESI-MS *m*/*z*: 946. The ^{13}C-NMR spectrum (CD_3OD, 600 MHz) showing the presence of eight methyl and three carbon atoms linked to oxygen and two alkenyl carbon atoms confirmed the structure. The ^{1}H-NMR and ^{13}C-NMR signals (Fig. 2D) were typical of protopanaxdiol glycoside. Chemical shift of C-3 and C-20 shifted to lower field, revealing the presence of the process of glycosylation. The result of TLC analysis showed that compound **4** and ginsenoside Rd standard have the same Rf value. Good agreement was obtained by the ^{1}H-NMR and ^{13}C-NMR spectrum with those reported in the literature.[30] Thus, the name ginsenoside Rd was given to compound **4**.

^{1}H-NMR and ^{13}C-NMR spectra of isolated compounds were given in Fig. 2, showing the atomic composition of each compound. The liquid chromatography of each compound, determined by a DIONEX P680 summit HPLC system with C18 column and ELSD detector, is attached with the NMR spectrum of the blank. The structural formulas of isolated compounds are shown in Fig. 3. The chemical shift is marked next to each atom, with a black numeral for hydrogen atom and a blue numeral for carbon atom.

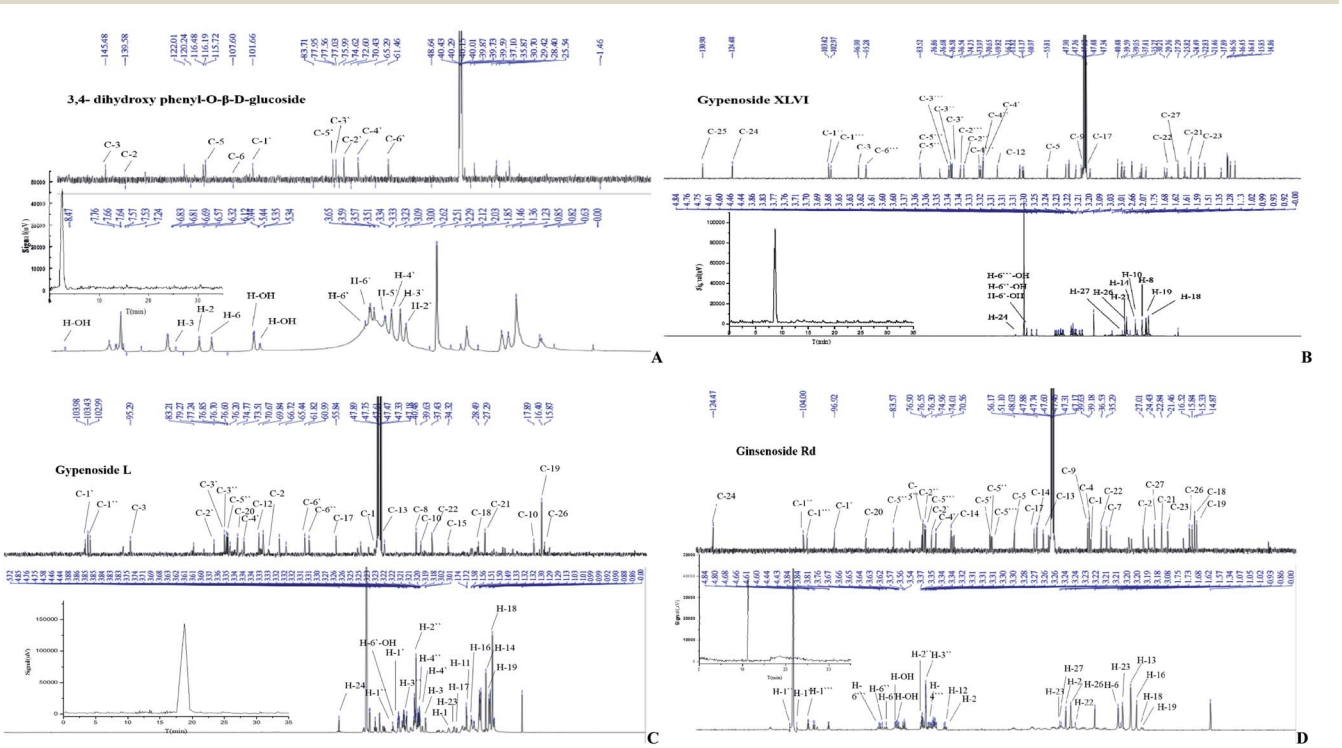

Fig. 2 NMR spectra and HPLC chromatographs of isolated compounds.

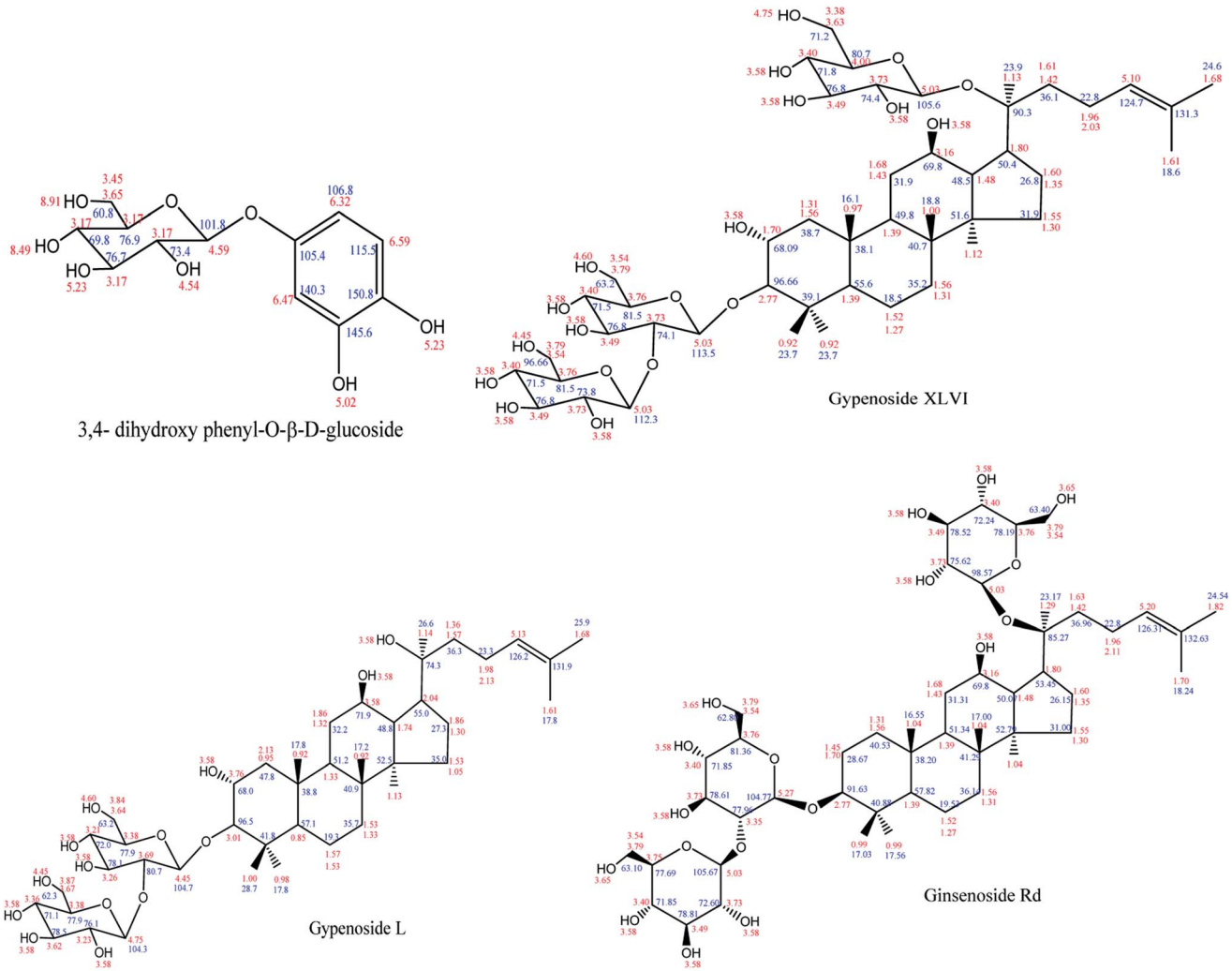

Fig. 3 Structure formula of isolated compounds.

3.2 DPPH scavenging capacity assay

The DPPH scavenging effect of all tested samples strongly depended on the given doses (Fig. 4A). The DPPH scavenging test of ethanol extract and its four polar fractions indicated that the DPPH clearance of five crude extracts at 800 μg mL^{-1} were 25.07% (ethanol extract), 19.38% (PE), 39.57% (EA), 24.35% (*n*-Bu) and 10.37 (W). Compared with the positive control, ethanol extract and its four polar fractions showed weaker scavenging capacity of the DPPH free radical. After the stepwise extraction of ethanol extract, the scavenging ability of four fractions to DPPH did not increase significantly. However, the scavenging ability of EA fraction and *n*-Bu fraction were significantly higher than that of ethanol extract, revealing the enrichment of compounds with antioxidant capacity to some extent. Therefore, EA fraction and *n*-Bu fraction were chosen to be further separated and purified.

3,4-Dihydroxy phenyl-*O*-β-D-glucoside showed outstanding scavenging ability to DPPH. Its scavenging ability reached 97.23% at 800 μg mL^{-1} and the IC_{50} was 63.52 μg mL^{-1}, more significant than the Vc. The DPPH scavenging ability of the four compounds followed the order: 3,4-dihydroxy phenyl-*O*-β-D-glucoside > gypenoside XLVI > gypenoside L > ginsenoside Rd. Furthermore, the scavenging capacity of gypenoside XLVI, gypenoside L and ginsenoside Rd at 800 μg mL^{-1} was 34.07%, 32.91%, and 38.64%, respectively, and was comparable to positive control (33.94%) at 25 μg mL^{-1}. The clearance of gypenoside XLVI and gypenoside L were almost alike at 25–800 μg mL^{-1}, which may be attributed to the triterpenoid sapogenin in their structure. 3,4-Dihydroxy phenyl-*O*-β-D-glucoside belongs to polyphenolic compounds and its hydrogen atoms of phenolic hydroxyls are highly unstable as they are usually excellent hydrogen or electron donors. Thus, 3,4-dihydroxy phenyl-*O*-β-D-glucoside might be responsible for the good DPPH scavenging ability of the EA fraction. Saponins have little influence on free radicals, but most of them can enhance the activity of antioxidant enzymes like superoxide dismutase (SOD) and catalase (CAT) in the body.[31] This might explain why gypenoside XLVI, gypenoside L and ginsenoside Rd showed suboptimal DPPH scavenging capacity.

3.3 ABTS scavenging capacity assay

All samples displayed the distinct ABTS scavenging effect in a dose-dependent relationship (Fig. 4B). Compared with the

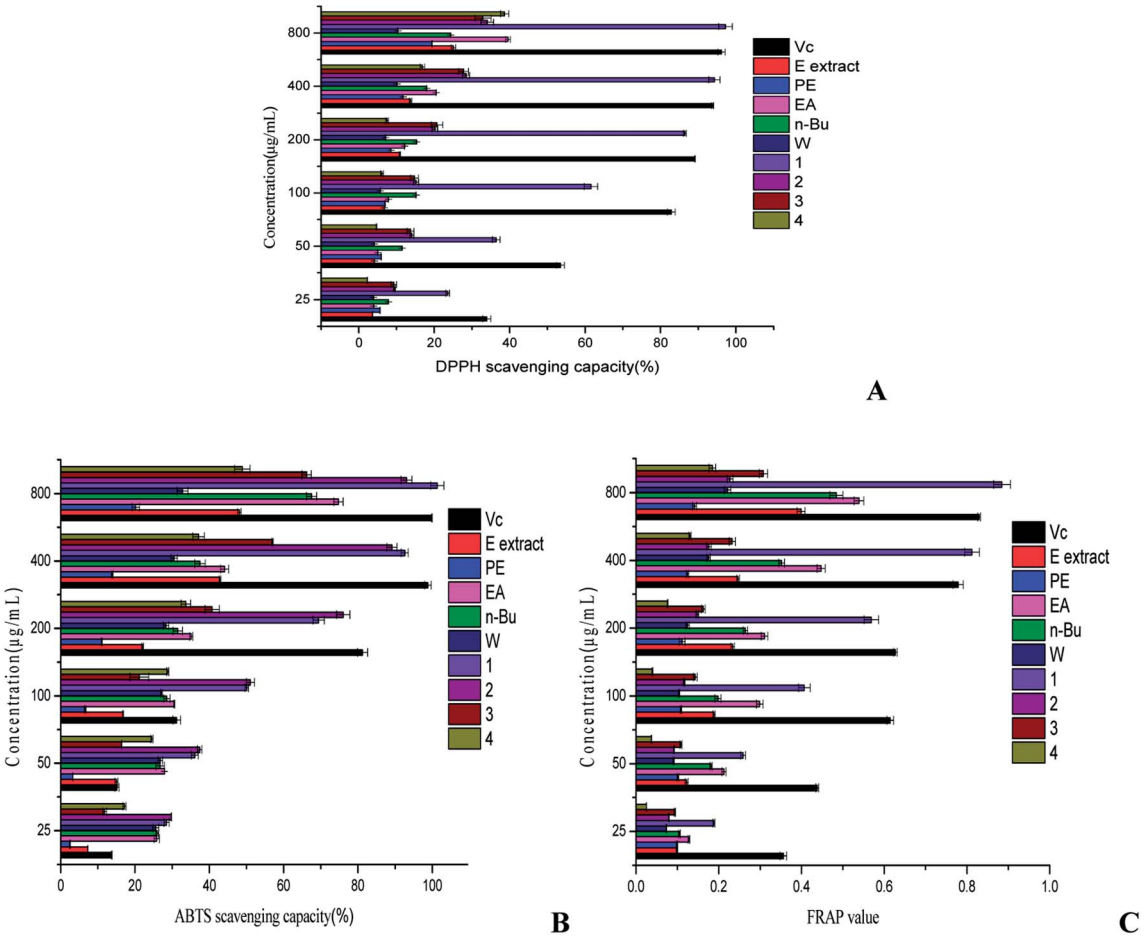

Fig. 4 Effects of all tested samples against oxidative stress. Three antioxidant assays were employed, including DPPH radical scavenging capacity (A), ABTS radical scavenging capacity (B) and ferric iron reducing antioxidant power (C).

positive control, EA fraction showed the most potent ABTS scavenging capacity. The ABTS scavenging ability of five crude extracts was in the following sequence: EA fraction > *n*-Bu fraction > ethanol extract > W fraction > PE. The ABTS scavenging rate of five crude extracts at 800 μg mL^{-1} were 48.09% (ethanol extract), 20.19% (PE), 74.77% (EA), 67.53% (*n*-Bu) and 32.81% (W). Collectively, as evidenced by the ABTS free radical scavenging capacities, the EA fraction and *n*-Bu fraction exhibited greater antioxidant potential.

The ABTS scavenging effect of the four compounds strongly depended on the given doses (Fig. 4B). The ABTS clearance of 3,4-dihydroxy phenyl-*O*-β-D-glucoside, gypenoside XLVI, gypenoside L and ginsenoside Rd at 800 μg mL^{-1} were 101.37%, 93.10%, 66.19% and 48.87%, respectively. 3,4-Dihydroxy phenyl-*O*-β-D-glucoside displayed the most outstanding scavenging capacity to ABTS. Its scavenging ability reached 101.37% at 800 μg mL^{-1} and the IC_{50} was 68.85 μg mL^{-1}, indicating that it had stronger scavenging ability than that of the control. The ABTS scavenging ability of four compounds were in the order: 3,4-dihydroxy phenyl-*O*-β-D-glucoside > gypenoside XLVI > gypenoside L > ginsenoside Rd. Considering that the antioxidant capacity of compounds originate from their unsaturated polyenoid system,[32] the adjacent phenolic hydroxyl of benzene ring of 3,4-dihydroxy phenyl-*O*-β-D-glucoside might have contributed to their strong ABTS scavenging effect. Gypenoside XLVI, gypenoside L and ginsenoside Rd, all of which are saponins, displayed different abilities in clearing the ABTS free radical. Studies have shown that the difference in the linking path and composition of the sugar chain leads to the difference in the biological activity of saponins.[33]

3.4 Ferric ion reducing antioxidant power (FRAP) assay

EA fraction and *n*-Bu fraction displayed better ferric ion reducing antioxidant power than the other crude extracts did, and their FRAP value at 800 μg mL^{-1} was 0.5389 and 0.4842, respectively, much lower than that of ascorbic acid (0.8294). Ferric reducing antioxidant powers of five crude extracts are arrayed in descending order as follows: EA, *n*-Bu, ethanol extract, W, PE, explaining the reason that the EA and *n*-Bu extracts were employed for further isolation and purification.

The FRAP value of 3,4-dihydroxy phenyl-*O*-β-D-glucoside, gypenoside XLVI, gypenoside L and ginsenoside Rd at 800 μg mL^{-1} reached 0.8846, 0.2273, 0.3078 and 0.1847, respectively (Fig. 4C). The ferric ion reducing antioxidant power of isolated compounds decreases in the following order: 3,4-dihydroxy phenyl-*O*-β-D-glucoside > gypenoside L > gypenoside XLVI > ginsenoside Rd. Due to the presence of an adjacent phenolic

hydroxyl, 3,4-dihydroxy phenyl-*O*-β-D-glucoside showed most significant ferric ion reducing power. The total reducing power of the three saponins is not ideal, which is in agreement with previously reported results.[34]

3.5 Cell viability of LO2

Drug-induced hepatotoxicity has become a very common complication caused by many medicines, because the liver is central to the metabolic disposition of virtually all drugs and exogenous compounds.[35] In the present research, the cytotoxicities of the five crude extracts and the four compounds were evaluated using LO2 cell lines (normal liver cell). Fig. 5 demonstrated that the cell viability of all samples was basically over 90%, showing almost no toxicity to LO2 cell lines. Therefore, the concentration range 25–800 μg mL^{-1} was selected for evaluating the anticancer properties of the samples.

3.6 Inhibition rate on MCF-7 cell proliferation

The inhibitory effects of crude extracts on MCF-7 cell proliferation are presented in Fig. 6. MCF-7 cells were intervened by different concentration of all samples. After 24 hours of intervention, the cell morphology and number were changed in varying degrees compared with the control group. The *n*-Bu fraction group presented the most obvious effect, showing a sharp reduction in the number of cells, larger intercellular space, numerous rounded cells, the free cellular debris and the decrease of cell anchoring rate. In EA and W fraction groups, the number of adherent cells and cell diopters decreased and some of the cells became round or had a long spindle shape. The inhibition rate of the five crude extracts at 800 μg mL^{-1} were 22.99%, 17.73%, 31.71%, 42.93% and 29.62%, respectively. Using the partitive extraction method, active components with anticancer abilities have been initially separated, mainly focusing on the EA fraction and *n*-Bu fraction.

The number of cells intervened by gypenoside L and ginsenoside Rd were greatly reduced, displaying an obvious cell gap, numerous round cells, decreased cell surface refractive index and visible broken cell debris. The density of cells interposed by 3,4-dihydroxy phenyl-*O*-β-D-glucoside and gypenoside XLVI decreased clearly, showing decreased cell diopter, increased suspended cells, rounding reduced cells and modified particles. The inhibition rate of 3,4-dihydroxy phenyl-*O*-β-D-glucoside, gypenoside XLVI, gypenoside L and ginsenoside Rd against MCF-7 cell lines at 800 μg mL^{-1} were 54.69%, 59.47%, 73.37% and 75.37%, respectively. 3,4-Dihydroxy phenyl-*O*-β-D-glucoside and gypenoside XLVI showed significant dose dependent effect, nearly equal to that showed by 5-fluorouracil. The effects of gypenoside L (IC_{50} 342.57 g mL^{-1}) and ginsenoside Rd (IC_{50} 432.31 g mL^{-1}) on the MCF-7 cell line were better than that of the positive control in a dose-dependent manner.

Structure–activity relationship studies have shown that the glycosylation moiety of saponins had an important contribution to cytotoxic activity.[36] One possible explanation is that gypenoside XLVI, gypenoside L and ginsenoside Rd all contain glycosyl groups that can directly destroy tumor cells and exert an anticancer effect.

3.7 Inhibition rate on A549 cell proliferation

The A549 cells in the control group were spindle or stellate shaped with well adherent-growth. However, cells in *n*-Bu fraction group became spherical, the diopter degraded, they shed easily, and cell proliferation was simultaneously down-regulated. The inhibitory experiment of crude extracts against A549 cell lines showed that the anticancer capacity of the five extract fractions followed the order: *n*-Bu fraction > PE fraction >

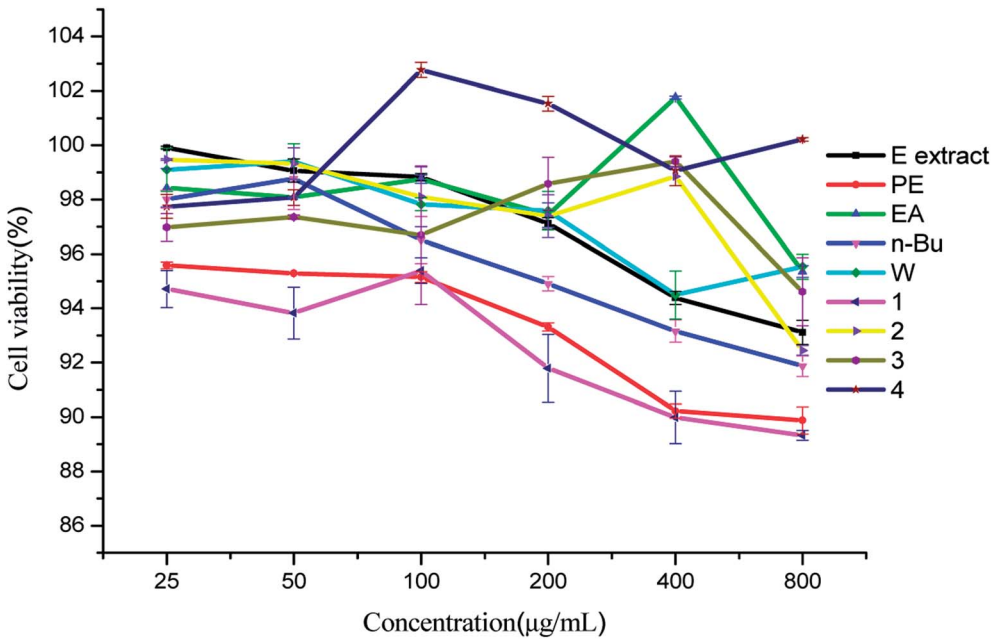

Fig. 5 Cell viability of LO2 cell lines treated with all tested samples.

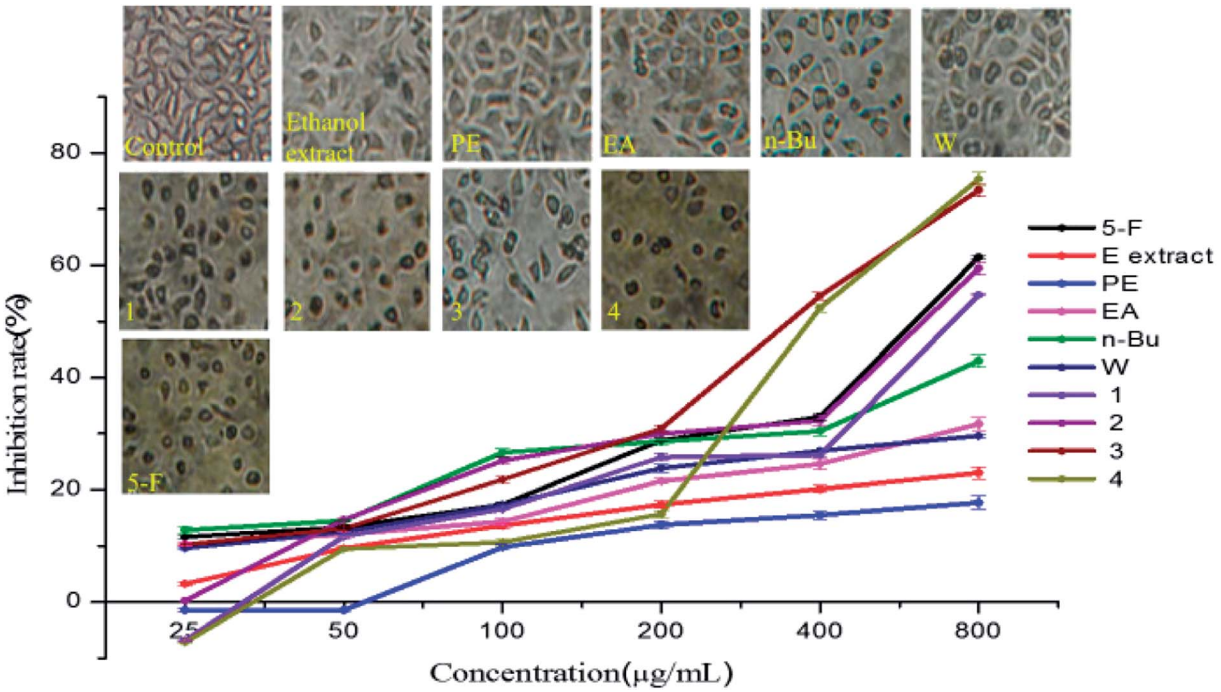

Fig. 6 Morphology effect and inhibition rate of all tested samples on MCF-7 cell lines.

EA fraction > W fraction > ethanol extract (Fig. 7). The *n*-Bu fraction displayed the most significant effect at 800 μg mL^{-1} (74.34%). The PE and EA fractions also showed certain anti-cancer ability in a concentration dependent manner.

For the isolated compounds, the ginsenoside Rd treated cells showed irregular cell morphology, unclear outlines, unclear contour, clouding margin and dissociated necrotic cell residues. The number of cells intervened by gypenoside L decreased greatly, and there was a greater internal gap between the cells which were accompanied by degraded cell diopter and visible broken cell debris. The cell density and volume treated by 3,4-dihydroxy phenyl-*O*-β-D-glucoside and gypenoside XLVI decreased and most of them became round, showing an increased suspended cells and cell debris and decreased cell refractive index. The inhibition rate of 3,4-dihydroxy phenyl-*O*-β-D-glucoside, gypenoside XLVI, gypenoside L and ginsenoside

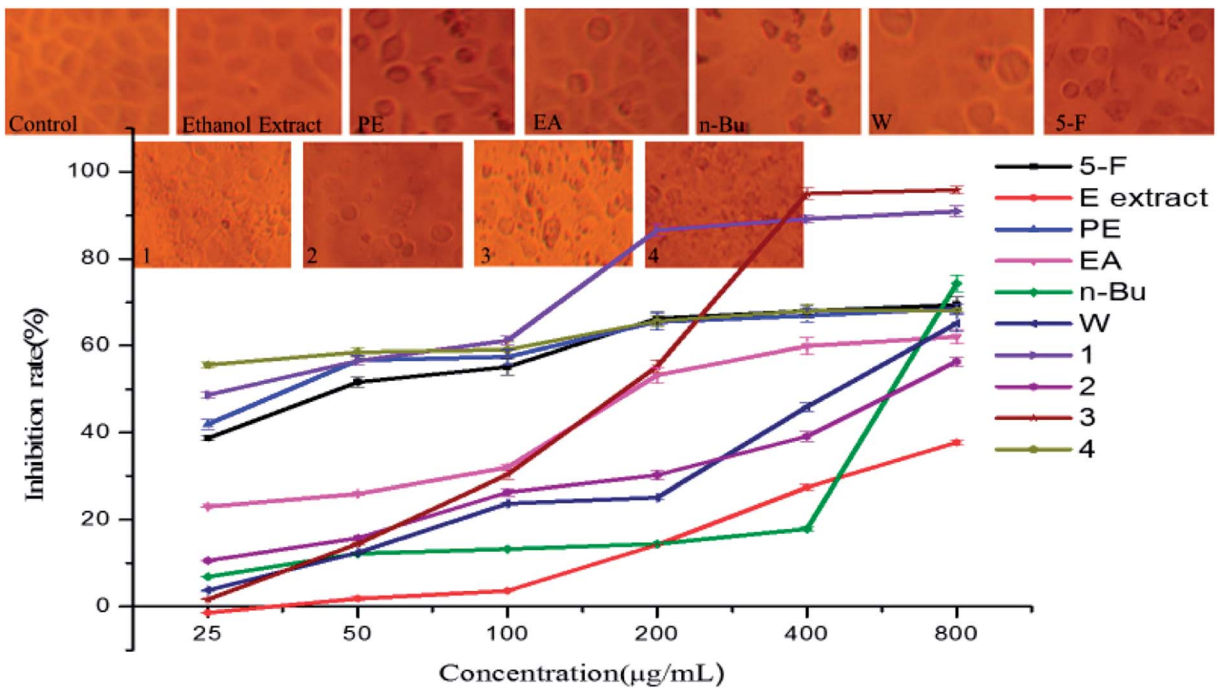

Fig. 7 Morphology effect and inhibition rate of all tested samples on A549 cell lines.

Rd at 800 μg mL^{-1} on A549 cells were 90.86%, 56.41%, 95.82% and 68.17%, respectively. The cancer cells were almost killed, especially in case of ginsenoside L.

It is obvious that 3,4-dihydroxy phenyl-*O*-β-D-glucoside inhibited tumor cell proliferation by enhancing the immunity and antioxidant ability of the body. Ordinarily, the pharmacological activity is relevant to chemical constitution. Previous research indicated that a free hydroxyl at the 20th or 21st carbon atom of dammarane-type saponin endows *G. pentaphyllum* saponins with significant anticancer ability.[37] Gypenoside XLVI, gypenoside L and ginsenoside Rd belong to dammarane-type saponins and none but the 20th carbon atom of gypenoside L have a free hydroxyl, which explains the activity discrepancy of the three saponins against A549 cell lines.

The antioxidant capacity or cytotoxicity of gypenosides from *G. pentaphyllum* were reported previously,[38,39] but the relationship between antioxidant and anticancer activities and related compounds has not been analyzed. The possibility of the antioxidant and anticancer activities being positively related was considered.[19] However, upon comparing the antioxidant and anticancer effects of all tested compounds in the present study, it was found that the strongest anticancer compound (Fig. 4) did not show the strongest antioxidant capacity (Fig. 6 and 7).

4. Conclusions

Four compounds with antioxidant and anticancer capacities were isolated from EA fraction and *n*-Bu fraction. 3,4-Dihydroxy phenyl-*O*-β-D-glucoside showed the highest antioxidant activity equivalent to vitamin C. Gypenoside L and ginsenoside Rd displayed the strongest anticancer capacity. Gypenoside L and ginsenoside Rd have a strong interference effect on the proliferation of A549 cell lines, which were better than that of 5-fluorouracil; yet, under similar conditions, they displayed ordinary effect against MCF-7 cell lines. The results implied that gypenoside L and ginsenoside Rd suppress tumor cell proliferation with a targeted characteristic. This study partially provided the material basis for the healthcare function of beverage products associated with *G. pentaphyllum*, combined with useful data for medical and pharmaceutical staff for the clinical application of *G. pentaphyllum*.

Conflicts of interest

There are no conflicts to declare.

Acknowledgements

This project was supported by Science and Technology Project of Guangzhou City (201604020150).

References

1 J. Liu, Y. Li, H. Shi, T. Wang, X. Wu, X. Sun and L. Yu, Components characterization of total tetraploid jiaogulan (*Gynostemma pentaphyllum*) saponin and its cholesterol-lowering properties, *J. Funct. Foods*, 2016, **23**, 542–555.

2 X. Zhang, G. Shi, Y. Sun, X. Wu and Y. Zhao, Triterpenes derived from hydrolyzate of total *Gynostemma pentaphyllum* saponins with anti-hepatic fibrosis and protective activity against H_2O_2-induced injury, *Phytochemistry*, 2017, **144**, 226–232.

3 Y. Niu, W. Yan, J. Lv, W. Yao and L. Yu, Characterization of a Novel Polysaccharide from Tetraploid *Gynostemma pentaphyllum* Makino, *J. Agric. Food Chem.*, 2013, **61**, 4882–4889.

4 F. Yang, H. Shi, X. Zhang, H. Yang, Q. Zhou and L. L. Yu, Two new saponins from tetraploid jiaogulan (*Gynostemma pentaphyllum*), and their anti-inflammatory and α-glucosidase inhibitory activities, *Food Chem.*, 2013, **141**, 3606–3613.

5 C. Zou, H. Shi, X. Liu, Y. Sheng, T. Ding, J. Yan, B. Gao, J. Liu, W. Lu and L. Yu, Conjugated linolenic acids and nutraceutical components in jiaogulan (*Gynostemma pentaphyllum*) seeds, *LWT–Food Sci. Technol.*, 2016, **68**, 111–118.

6 X. Zhuohong, H. Haiqiu, Z. Yang, S. Haiming, W. Shaoke, T. T. Y. Wang, C. Pei and Y. Liangli Lucy, Chemical composition and anti-proliferative and anti-inflammatory effects of the leaf and whole-plant samples of diploid and tetraploid *Gynostemma pentaphyllum* (Thunb.) Makino, *Food Chem.*, 2012, **132**, 125–133.

7 J. C. Chen, T. Chinchuan, L. D. Chen, H. H. Chen and W. C. Wang, Therapeutic effect of gypenoside on chronic liver injury and fibrosis induced by CCl_4 in rats, *Am. J. Chin. Med.*, 2000, **28**, 175–185.

8 C. C. Lin, P. C. Huang and J. M. Lin, Antioxidant and hepatoprotective effects of *Anoectochilus formosanus* and *Gynostemma pentaphyllum*, *Am. J. Chin. Med.*, 2000, **28**, 87.

9 R. Gauhar, S. L. Hwang, S. S. Jeong, J. E. Kim, H. Song, D. C. Park, K. S. Song, T. Y. Kim, W. K. Oh and T. L. Huh, Heat-processed *Gynostemma pentaphyllum* extract improves obesity in ob/ob mice by activating AMP-activated protein kinase, *Biotechnol. Lett.*, 2012, **34**, 1607–1616.

10 L. Chianjiun, W. C. Huang, K. Mingling, R. C. Yang and J. J. Shen, Long-term oral administration of *Gynostemma pentaphyllum* extract attenuates airway inflammation and Th2 cell activities in ovalbumin-sensitized mice, *Food Chem. Toxicol.*, 2010, **48**, 2592–2598.

11 S. Megalli, F. Aktan, N. M. Davies and B. D. Roufogalis, Phytopreventative anti-hyperlipidemic effects of *Gynostemma pentaphyllum* in rats, *J. Pharm. Pharm. Sci.*, 2005, **8**, 507.

12 A. Norberg, N. K. Hoa, E. Liepinsh, P. D. Van, N. D. Thuan, H. Jörnvall, R. Sillard and C. G. Ostenson, A novel insulin-releasing substance, phanoside, from the plant *Gynostemma pentaphyllum*, *J. Biol. Chem.*, 2004, **279**, 41361–41367.

13 T. C. Cheng, J. F. Lu, J. S. Wang, L. J. Lin, H. Kuo and B. H. Chen, Antiproliferation Effect and Apoptosis Mechanism of Prostate Cancer Cell PC-3 by Flavonoids and Saponins Prepared from *Gynostemma pentaphyllum*, *J. Agric. Food Chem.*, 2011, **59**, 11319–11329.

14 P. Poprac, K. Jomova, M. Simunkova, V. Kollar, C. J. Rhodes and M. Valko, Targeting Free Radicals in Oxidative Stress-Related Human Diseases, *Trends Pharmacol. Sci.*, 2017, **38**, 592–607.

15 P. Sivaguru, K. Parameswaran and A. Lalitha, Antioxidant, anticancer and electrochemical redox properties of new bis(2,3-dihydroquinazolin-4(1*H*)-one) derivatives, *Mol. Diversity*, 2017, 1–10.

16 O. Parésbadell, M. Banqué, F. Macià, X. Castells and M. Sala, Impact of comorbidity on survival by tumour location: breast, colorectal and lung cancer (2000-2014), *Cancer Epidemiol.*, 2017, **49**, 66–74.

17 R. K. Khurana, A. Jain, A. Jain, T. Sharma, B. Singh and P. Kesharwani, Administration of antioxidants in cancer: debate of the decade, *Drug Discovery Today*, 2018, **23**, 763–770.

18 J. N. Moloney and T. G. Cotter, ROS signalling in the biology of cancer, *Semin. Cell Dev. Biol.*, 2017, DOI: 10.1016/j.semcdb.2017.05.023.

19 N. M. Al-Enazi, A. S. Awaad, M. E. Zain and S. I. Alqasoumi, Antimicrobial, antioxidant and anticancer activities of *Laurencia catarinensis*, *Laurencia majuscula* and *Padina pavonica* extracts, *Saudi Pharm. J.*, 2017, **26**, 44–52.

20 S. M. Ivanov, A. A. Lagunin and V. V. Poroikov, In silico assessment of adverse drug reactions and associated mechanisms, *Drug Discovery Today*, 2015, **21**, 58–71.

21 A. Gurib-Fakim, Medicinal plants: traditions of yesterday and drugs of tomorrow, *Mol. Aspects Med.*, 2006, **27**, 1–93.

22 J. G. Jiang, X. J. Huang, J. Chen and Q. S. Lin, Comparison of the sedative and hypnotic effects of flavonoids, saponins, and polysaccharides extracted from Semen *Ziziphus jujube*, *Nat. Prod. Res.*, 2007, **21**, 310–320.

23 Q. H. Zeng, J. B. Zhao, J. J. Wang, X. W. Zhang and J. G. Jiang, Comparative extraction processes, volatile compounds analysis and antioxidant activities of essential oils from *Cirsium japonicum* Fisch. ex DC and *Cirsium setosum* (Willd.) M.Bieb, *LWT–Food Sci. Technol.*, 2016, **68**, 595–605.

24 R. Re, N. Pellegrini, A. Proteggente, A. Pannala, M. Yang and C. RiceEvans, Antioxidant activity applying an improved ABTS radical cation decolorization assay, *Free Radical Biol. Med.*, 1999, **26**, 1231.

25 I. F. Benzie and J. J. Strain, The Ferric Reducing Ability of Plasma (FRAP) as a Measure of "Antioxidant Power": The FRAP Assay, *Anal. Biochem.*, 1996, **239**, 70–76.

26 C. Y. Shen, J. G. Jiang, M. Q. Li, C. Y. Zheng and W. Zhu, Structural characterization and immunomodulatory activity of novel polysaccharides from Citrus aurantium Linn. variant amara Engl, *J. Funct. Foods*, 2017, **35**, 352–362.

27 L. Verotta, F. Orsini, F. Pelizzoni, G. Torri and C. B. Rogers, Polyphenolic Glycosides from African Proteaceae, *J. Nat. Prod.*, 1999, **62**, 1526.

28 T. Takemoto, S. Arihara, T. Nakajima and M. Okuhira, Studies on the Constituents of *Gynostemma pentaphyllum* Makino. II. Structures of Gypenoside XV-XXI, *J. Pharm. Soc. Jpn.*, 1983, **103**, 1015–1023.

29 D. J. Chen, H. M. Liu, S. F. Xing and X. L. Piao, Cytotoxic activity of gypenosides and gynogenin against non-small cell lung carcinoma A549 cells, *Bioorg. Med. Chem. Lett.*, 2014, **24**, 186–191.

30 X. Zhao, J. Wang, J. Li, L. Fu, J. Gao, X. Du, H. Bi, Y. Zhou and G. Tai, Highly selective biotransformation of ginsenoside Rb1 to Rd by the phytopathogenic fungus *Cladosporium fulvum* (syn. *Fulvia fulva*), *J. Ind. Microbiol. Biotechnol.*, 2009, **36**, 721–726.

31 S. G. Sparg, M. E. Light and J. V. Staden, Biological activities and distribution of plant saponins, *J. Ethnopharmacol.*, 2004, **94**, 219.

32 C. Y. Shen, W. L. Zhang and J. G. Jiang, Immune-enhancing activity of polysaccharides from Hibiscus sabdariffa Linn. via MAPK and NF-kappa B signaling pathways in RAW264.7 cells, *J. Funct. Foods*, 2017, **34**, 118–129.

33 M. Chwalek, K. Plé and L. Voutquenne-Nazabadioko, Synthesis and hemolytic activity of some hederagenin diglycosides, *Chem. Pharm. Bull.*, 2004, **52**, 965.

34 Y. S. Jing, L. F. Wu, Z. D. Zhang and Y. Juan, Evaluation on antioxidant activities of extracts from *Gynostemma Pentaphyllum*, *Journal of Mountain Agriculture and Biology*, 2010, **29**, 43–47.

35 A. I. Shehu, X. Ma and R. Venkataramanan, Mechanisms of Drug-Induced Hepatotoxicity, *Clin Liver Dis*, 2017, **21**, 35–54.

36 Z. Y. Yu and H. Yang, Recent research on *Gynostemma pentaphyllum*, *Chin. Pharm. J.*, 1988, **23**, 12–14.

37 Q. Lu, J. G. Cao and Q. Ke, Susceptibility test of leukemic cells to *Gynostemma Pentaphyllum* saponins, *Medical Science Journal of Central South China*, 1993, 386–387.

38 W. Jiang, H. Shan, J. Song and H. Lü, Separation and Purification of Ombuoside from *Gynostemma Pentaphyllum* by Microwave-Assisted Extraction Coupled with High-Speed Counter-current Chromatography, *J. Chromatogr. Sci.*, 2017, **55**, 69–74.

39 S. F. Xing, L. H. Liu, M. L. Zu, X. F. Ding, W. Y. Cui, T. Chang and X. L. Piao, The inhibitory effect of gypenoside stereoisomers, gypenoside L and gypenoside LI, isolated from *Gynostemma pentaphyllum* on the growth of human lung cancer A549 cells, *J. Ethnopharmacol.*, 2018, 161–172.

